

# Measurement of Surface Shear Stress Vectors Using Liquid Crystal Coatings

Daniel C. Reda\* and Joseph J. Muratore Jr.†

NASA Ames Research Center, Moffett Field, California 94035

Under normal white light illumination and oblique observation, liquid crystal coating (LCC) color-change response to shear depends on both shear stress magnitude as well as the direction of the applied shear relative to the observer's line of sight. These color-change responses were quantified by subjecting a LCC to a wall-jet shear flow and measuring scattered-light spectra using a fiber optic probe and spectrophotometer. At any fixed shear stress magnitude, the maximum color change was measured when the shear vector was aligned with and directed away from the observer; changes in the relative in-plane view angle to either side of this vector/observer aligned position resulted in symmetric Gaussian reductions in measured color change. Based on these results, a surface shear stress vector measurement methodology, involving multiple oblique-view observations of the test surface, was formulated. Under present test conditions, the measurement resolution of this technique was found to be  $\pm 1$  deg for vector orientations and  $\pm 5\%$  for vector magnitudes. An approach to extend the present methodology to full-surface applications is proposed.

## Nomenclature

$C_f$	= skin friction coefficient
$D$	= jet exit diameter
$I$	= spectral scattering intensity
$N$	= number of data points used in curve fits or in data-reduction technique
$V$	= velocity
$W$	= white light
$X, Y$	= chromaticity coordinates
$\alpha$	= above-plane view angle, measured positive upward from zero in plane of test surface
$\beta$	= relative circumferential-view angle in plane of test surface measured between observer line of sight and shear vector (positive clockwise)
$\Delta P$	= pressure difference used to drive jet flow
$\lambda$	= wavelength of light
$\lambda_D$	= dominant wavelength
$\rho$	= density
$\tau$	= magnitude of surface shear stress vector
$\phi$	= circumferential angle in plane of test surface, measured positive counterclockwise from origin
$\phi_t$	= orientation of surface shear stress vector, directed away from observer with line-of-sight at $\phi = \phi_t$

## Subscripts

$C$	= camera
$J$	= jet
$L$	= light
$P$	= probe
$r$	= reference value

## Introduction

THE objective of the present research is to develop a technique for the areal measurement of the surface shear stress distribu-

tion acting on any test surface immersed in a three-dimensional flowfield. In fundamental experiments, full-surface measurements of both the magnitudes and the directions of such skin-friction forces would provide modelers with detailed data sets for code-validation purposes, ultimately leading to more advanced design tools. Once proven, the application of such a measurement capability to the prototype testing of advanced aerodynamic configurations could greatly increase the productivity of ground-based facilities.

A review of the state of the art<sup>1-3</sup> shows that numerous point-measurement techniques are currently available to determine surface shear stress magnitude; several of these methods can also be used to measure local shear stress direction. However, no full-surface, vector-measurement capability presently exists. The method presented here demonstrates that both the magnitude and direction of surface shear stress vectors can be accurately quantified from measurements of the color-change response of liquid crystal coatings subjected to such shearing forces. An approach to extend the present point-measurement method to a full-surface technique is outlined.

## Liquid Crystals

Cholesteric liquid crystals reside in a highly anisotropic mesophase that exists between the solid and isotropic-liquid phases of some organic compounds.<sup>4</sup> Such materials can exhibit birefringent optical properties that are characteristic of a crystalline solid state. Once aligned by shear, molecules within a thin liquid crystal coating scatter incident white light as a spectrum of colors, with each color at a different orientation relative to the surface. Shear stress sensitive and temperature insensitive compounds now exist; one such compound, Hallcrest mixture CN/R3, was used in the present research. For such coatings, "color play," i.e., discerned color changes at a fixed angle of observation for a fixed angle of illumination, results solely from the application of shear stress. Such color changes are continuous and reversible, with time response of order milliseconds. Based on these characteristics, liquid crystal coatings have been used to visualize shear stress patterns on aerodynamic surfaces in both laboratory<sup>5-8</sup> and flight-test<sup>9</sup> applications.

Initial attempts at using liquid crystal mixtures available in the late 1960s to measure surface shear stress magnitude were not successful.<sup>10</sup> Recently, however, two major advances in the liquid crystal method were achieved that demonstrated its potential use as a measurement technique. First, under carefully controlled laboratory conditions, quantitative calibrations between observed color changes and changes in surface shear stress magnitude were shown to be possible.<sup>11-15</sup> Second, Reda et al.<sup>16</sup> have shown that,

Received Dec. 22, 1993; presented as Paper 94-0729 at the AIAA 32nd Aerospace Sciences Meeting, Reno, NV, Jan. 10-13, 1994; revision received April 11, 1994; accepted for publication April 20, 1994. Copyright © 1994 by the American Institute of Aeronautics and Astronautics, Inc. No copyright is asserted in the United States under Title 17, U.S. Code. The U.S. Government has a royalty-free license to exercise all rights under the copyright claimed herein for Governmental purposes. All other rights are reserved by the copyright owner.

\*Senior Research Scientist, Fluid Mechanics Laboratory Branch. Associate Fellow AIAA.

†Research Assistant, MCAT Institute; currently Imaging Engineer, IK Systems, Pittsford, NY 14534.

for a fixed observer, equal magnitude but opposite direction shear vectors applied to a liquid crystal coating cause different color-play responses. Therefore, the present understanding is that liquid crystal color-play response depends on both shear stress magnitude and direction. This paper describes how this newly acquired knowledge was utilized to convert the liquid crystal coating method from a flow-visualization tool into a quantitative technique for the measurement of surface shear stress vectors.

### Coating Application Technique

In fluid-mechanics applications, a mixture of one part liquid crystals to nine parts of a solvent such as Freon is sprayed onto the aerodynamic surface under study. For small test areas, an artist airbrush is the preferred spray tool. A smooth, flat-black surface is essential for color contrast, and it must be kept free of grease and other chemical contaminants. Recommended applications after spray losses are 10–20 ml of liquid crystals, measured prior to mixing with the solvent, onto each square meter of surface area. The solvent evaporates, leaving a uniform thin film of liquid crystals whose thickness, based on mass conservation and estimated spray losses, is approximately 10–20  $\mu\text{m}$  (0.0004–0.0008 in.).

The molecules within a newly sprayed coating are generally not aligned in the planar/layered orientation<sup>4</sup> required to disperse white light into a spectrum of colors. When recording full-surface

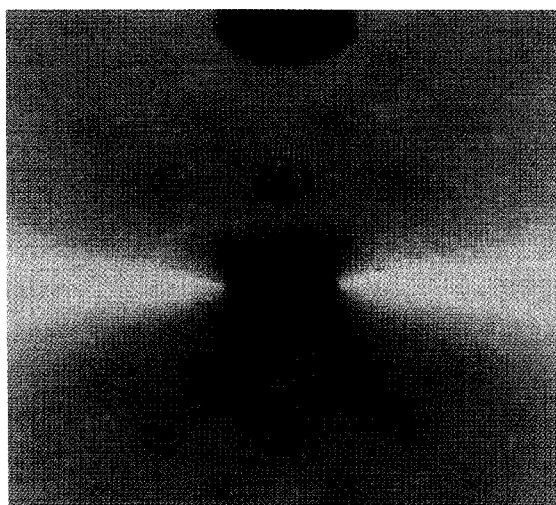


Fig. 1 Color-play response of liquid crystal coating to normal jet impingement under normal white-light illumination ( $\alpha_c = 35$  deg;  $0 \leq \phi_c \leq 360$  deg).

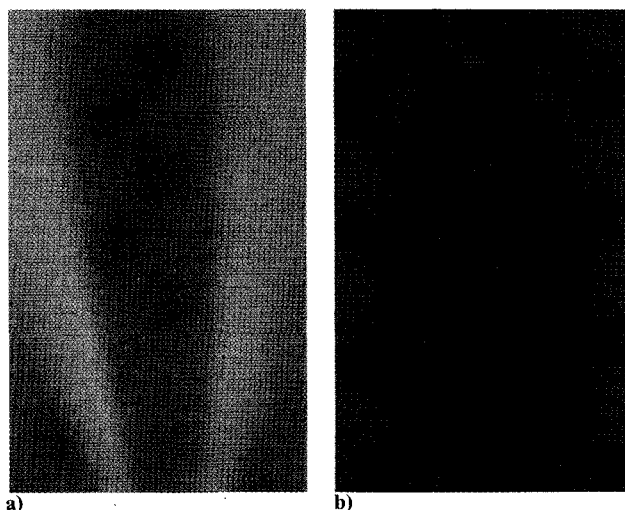


Fig. 2 Color-play response of liquid crystal coating to tangential jet flow under normal white-light illumination,  $\alpha_c = 35$  deg: a) flow away from observer and b) flow toward observer.

color video images, molecules within the coating were prealigned by shear into the color-play state by the passage of an oblique/multidirectional pressurized airstream over the test surface. This procedure rendered the no-shear or “background” color visible. For the spectral measurements, the highest shear level of the tangential jet itself was used to align the liquid crystal molecules before data were acquired.

### Color Video Images

Two simple flowfields were used in the present research to impose surface shear stress vectors on the liquid crystal coating. First, to demonstrate the sensitivity of such coatings to shear stress direction, a circular jet of air was impinged normal to a planar test surface. The liquid crystal coating was illuminated with white light also directed normal to the test surface. A color video camera positioned at an above-plane view angle,  $\alpha_c = 35$  deg, was rotated about the center of the test plate in a manner such that the coating color-play response to shear could be recorded at any circumferential-view angle  $\phi_c$ . Figure 1 shows a color video image that universally characterizes the coating response to this flow.

At any specified radial distance from its stagnation point, a circular jet impinging normal to a flat surface imposes equal-magnitude shear vectors on the coating in all radial directions. In marked contrast to earlier studies which incorporated oblique illumination,<sup>16</sup> here, under normal illumination, any point exposed to a shear vector with a component directed away from the observer exhibited a color-play response, i.e., a shift from the no-shear orange color toward the blue end of the visible spectrum. Conversely, any point exposed to a shear vector with a component directed toward the observer exhibited a noncolor-play response, always characterized by a rusty red or brown appearance independent of shear magnitude. Equally as important, this two-lobe color pattern was seen to rotate with the observer, i.e., it was identically oriented relative to the observer for all circumferential-view angles.

The normal jet of air was then repositioned to blow tangentially across the test surface. Figure 2 shows two color images of the coating response to this flowfield, the first for flow directed away from the observer, the second for flow directed toward the observer. These color-play and noncolor-play responses are entirely consistent with the radial-flow results.

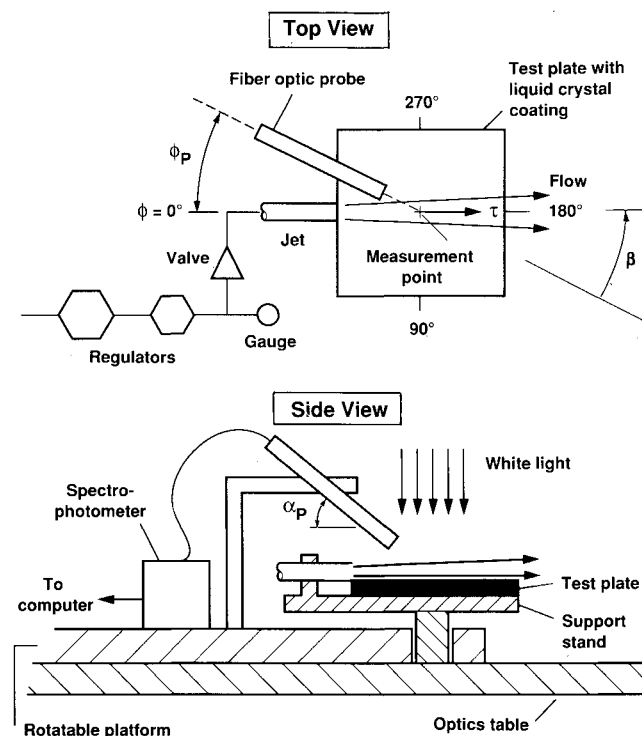


Fig. 3 Schematic of experimental arrangement.

### Experimental Arrangement

The experimental arrangement shown in Fig. 3 was devised to quantify the liquid crystal color-play responses to shear illustrated in Figs. 1 and 2. A tangential jet of air ( $D = 0.33$  in. and  $250 \leq V_j \leq 750$  ft/s) was blown across a liquid crystal coated planar test surface (a  $5 \times 5$ -in. plate). The pressure difference used to drive this flow was controlled by two pressure regulators in series, and its value was indicated by a calibrated gauge. In such wall jet flows, the skin-friction coefficient

$$C_f = \frac{\tau}{(1/2)\rho V_j^2} \quad (1)$$

is essentially constant in the near-exit region over a broad range of Reynolds numbers.<sup>17</sup> Thus,

$$\frac{\tau}{\tau_r} = \frac{\rho V_j^2}{\rho_r V_{j,r}^2} \quad (2)$$

where subscript  $r$  denotes an arbitrary lowest shear reference level.

In the limit of incompressible, inviscid flow within the jet delivery system between the gauge and the jet exit,

$$\Delta P = (1/2)\rho V_j^2 \quad (3)$$

or

$$\frac{\Delta P}{\Delta P_r} = \frac{\rho V_j^2}{\rho_r V_{j,r}^2} \quad (4)$$

where subscript  $r$  denotes the pressure difference at the lowest shear reference condition. Combining Eqs. (2) and (4) yields

$$\frac{\Delta P}{\Delta P_r} = \frac{\tau}{\tau_r} \quad (5)$$

No attempts were made in these proof-of-concept experiments to measure absolute wall shear stress magnitudes, hence Eq. (5) was not verified directly. The scaling relationship of Eq. (4) was checked experimentally, by measuring centerline velocities at the jet exit with a miniature pitot probe, and shown to be valid. Therefore, based on the combined data of Ref. 17 and present measurements, Eq. (5) was used to set the five parametric, integer values of relative surface shear stress magnitude,  $\tau/\tau_r = 1, 2, 4, 6$ , and  $8$ , for this study. A similar approach was recently employed by Parmar.<sup>18</sup> The absolute surface shear stress range for the present experiments was estimated<sup>17</sup> to be  $0.3$ – $2.6$  psf.

The issue of the relative in-plane view angle between the color-measuring device and the shear vector will now be addressed. A fiber optic probe at  $\alpha_p = 30^\circ$  was used to capture light scattered from a point on the centerline of the wall jet flow. The effective sampling diameter of this sensor was order  $0.10$  in. The measurement point was always coincident with the center of rotation of the probe-traversing system thereby allowing the relative in-plane view angle between the shear vector and the observer  $\beta$  to be systematically varied. Note that the  $\beta = 0$ -deg orientation corresponds to the case where the shear vector is aligned with and directed away from the observer. Light captured by the probe was input to a spectrophotometer (Oriol Instaspec II diode array system) which dispersed it into its spectral content. Measurements of scattering intensity from the coating as a function of the wavelength of light were thus obtained over the entire visible spectrum.

### Spectral Measurements

Normal white light (5600 K) was supplied from a NAC Visual Systems HMI-1200 unit incorporating a 1200-W Sylvania PAR64 BriteBeam source with an ultraviolet filter and a flicker-free ballast. The intensity/wavelength distribution for this light source is shown in Fig. 4. The mean intensity level is seen to be relatively

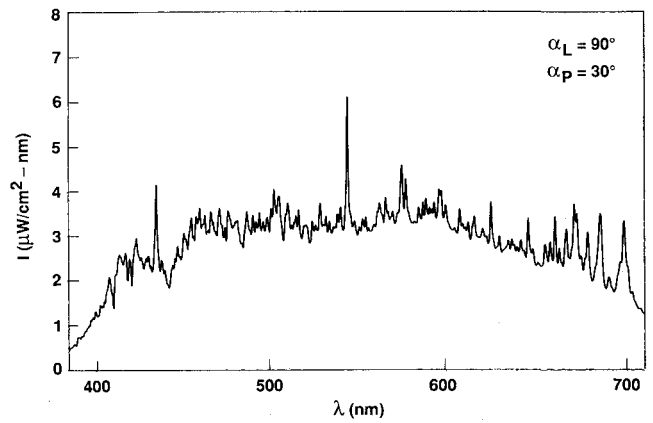


Fig. 4 White-light spectrum; scattering intensity vs wavelength.

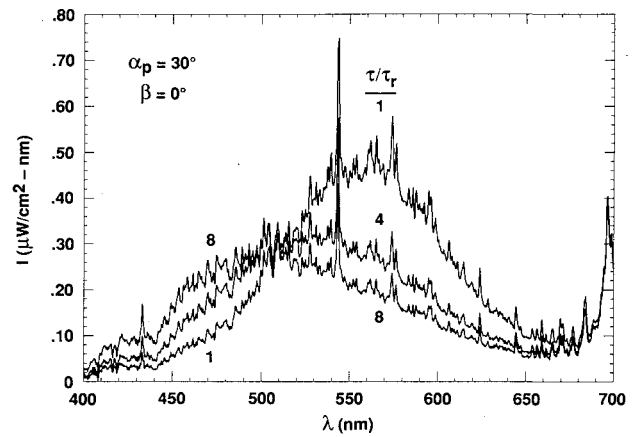


Fig. 5 Liquid crystal coating spectra; scattering intensity vs wavelength for flow away from the observer, with relative surface shear stress magnitude as the parameter.

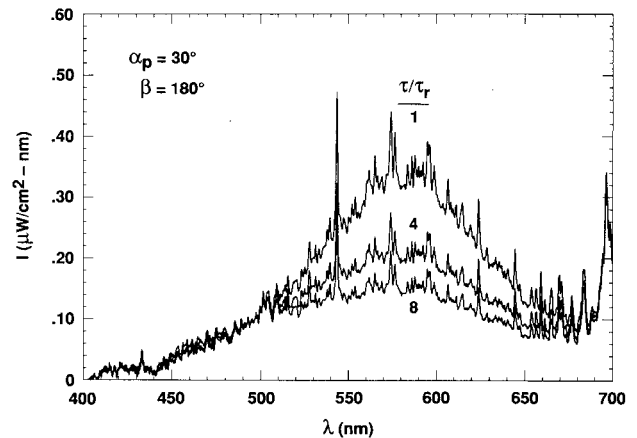


Fig. 6 Liquid crystal coating spectra; scattering intensity vs wavelength for flow toward the observer, with relative surface shear stress magnitude as the parameter.

constant over the visible spectrum. The pronounced spikes are a characteristic of the light source itself and will be seen to reoccur at these fixed, discrete wavelengths in all subsequent spectra.

Figure 5 shows measured liquid crystal coating spectra for the case of flow directly away from the observer, with relative surface shear stress magnitude as the parameter. As shear magnitude was increased, the peak intensity of the scattered light was seen to decrease. More importantly, the wavelength corresponding to this peak intensity was seen to shift to lower wavelengths, indicating a shift in color from orange, through yellow and green, to blue.

Figure 6 shows measured liquid crystal coating spectra for the case of flow directly toward the observer, again with relative sur-

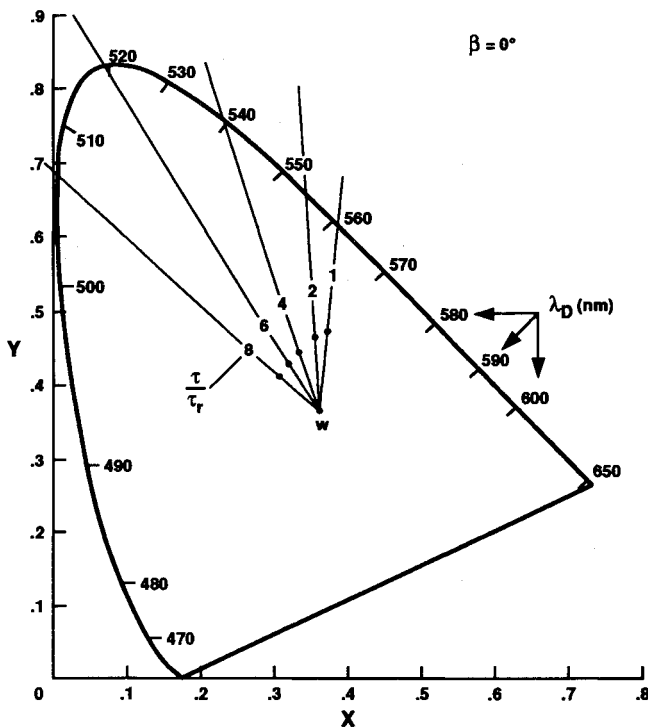


Fig. 7 Dependence of liquid crystal chromaticity coordinates on relative surface shear stress magnitude at  $\beta = 0^\circ$ ; graphical determination of dominant wavelengths.

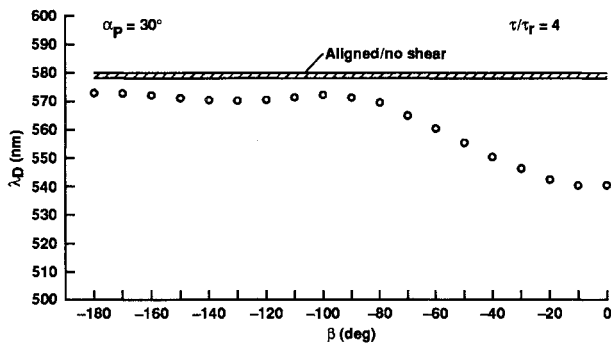


Fig. 8 Dominant wavelength vs relative circumferential-view angle between observer and shear vector; example of color-play and non-color-play regimes.

face shear stress magnitude as the parameter. Here, in marked contrast to the results of Fig. 5, as shear magnitude was increased, the peak intensity of the scattered light decreased, but no shift in the wavelength corresponding to this peak intensity was measured, i.e., no color change occurred.

To determine the color of the coating at each test condition, scattering intensity spectra were converted into standard chromaticity coordinates (X, Y) using established methods.<sup>19-21</sup> This procedure involves integration of the measured spectra over the visible wavelength regime, factoring in the characteristics of the illumination source and the standard human eye response to color change. Results for  $\beta = 0^\circ$  are shown in Fig. 7, where an empirically defined relationship between the color of the liquid crystal coating and the relative magnitude of the shear stress applied to it is clearly shown. Dominant wavelengths  $\lambda_D$ , obtained by extrapolation from white light W through the measured chromaticity coordinates (solid dots) to the extremes of the chromaticity diagram, were found to be entirely consistent with the observed peak-power wavelengths of Fig. 5 and the color image of Fig. 2a.

Figure 8 shows a plot of measured dominant wavelength as a function of relative in-plane view angle between the probe line of sight and the shear vector over the complete range  $-180 \leq \beta \leq 0^\circ$ ; relative surface shear stress magnitude is held constant at 4. As

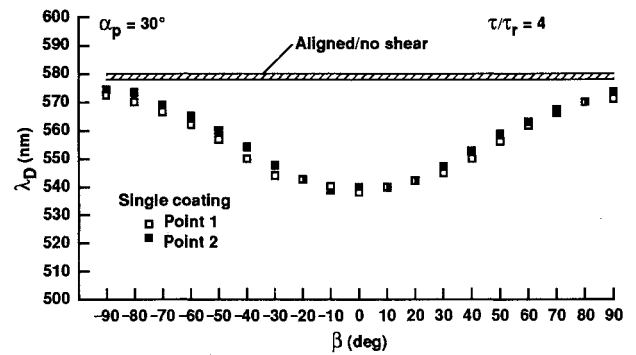


Fig. 9 Dominant wavelength vs relative circumferential-view angle between observer and shear vector; example of point-to-point variations for a single coating.

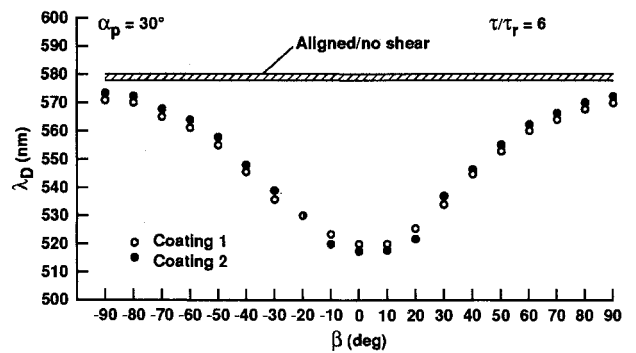


Fig. 10 Dominant wavelength vs relative circumferential-view angle between observer and shear vector; example of coating-to-coating variations.

the probe line of sight was rotated from  $\beta = 0^\circ$  toward  $\beta = -90^\circ$  deg, a continuous increase in  $\lambda_D$  was recorded, thereby defining the color-play regime. However, in the quadrant  $-180 \leq \beta \leq -90^\circ$  deg, no additional change in  $\lambda_D$  was recorded, thereby defining the non-color-play regime. As noted with Fig. 1, only shear vectors with components directed away from the observer cause a color-play response.

Concerning repeatability of such measurements, Fig. 9 illustrates point-to-point variations in the  $\lambda_D$  vs  $\beta$  color-play response of a single coating exposed to a fixed shear value of  $\tau/\tau_r = 4$ . The two measurement points were widely spaced such that the shear pattern of the first exposure and the shear pattern of the second exposure did not overlap. Such measurements were generally repeated to within 2–3 nm. Figure 10 illustrates coating-to-coating variations at a fixed shear level of  $\tau/\tau_r = 6$ . Repeatability of  $\lambda_D$  values to within 2–3 nm also was achieved here. Similar small variations in  $\lambda_D$ , of  $\sim 2$  nm, were measured after 6-min exposures to the highest relative shear value of  $\tau/\tau_r = 8$ , indicating that coating degradation is not a critical issue when mixtures are properly selected to be compatible with the shear levels encountered.

### Proof-of-Concept Results

Figures 11 and 12 summarize the present proof-of-concept measurements. Figure 11 shows an ensemble plot of  $\lambda_D$  vs  $\beta$  for data taken throughout the color-play regime ( $-90 \leq \beta \leq 90^\circ$ ) with relative surface shear stress magnitude as the parameter. Two principal results are evident: 1) for a given shear stress magnitude, the minimum dominant wavelength, i.e., the maximum color change, is measured when the shear vector is aligned with, and directed away from, the observer ( $\beta = 0^\circ$ ); and 2) for a given shear stress magnitude, changes in relative circumferential-view angle  $\beta$  to either side of the vector/observer aligned position result in symmetric increases in measured dominant wavelength. Furthermore, it was found that each of these measured data sets could be well fit by a Gaussian curve for  $-90 \leq \beta \leq 90^\circ$  deg, or, as will be demonstrated shortly, by a simple second-order polynomial curve over the limited range  $-60 \leq \beta \leq 60^\circ$  deg.

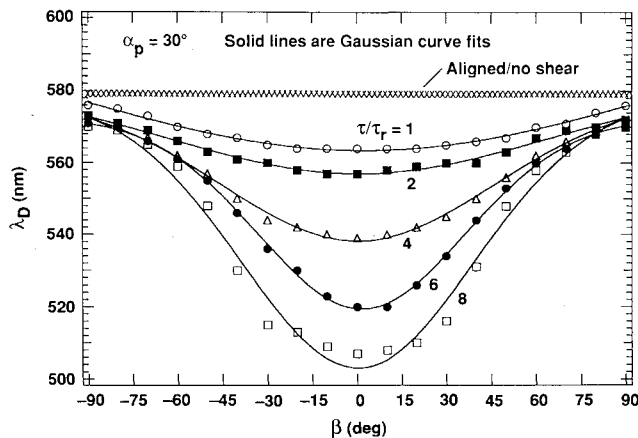


Fig. 11 Dominant wavelength vs relative circumferential-view angle between observer and shear vector, with relative surface shear stress magnitude as the parameter.

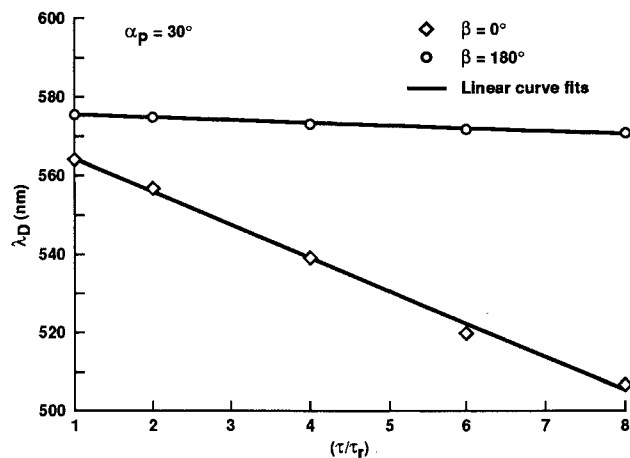


Fig. 12 Dominant wavelength vs relative surface shear stress magnitude for limiting circumferential-view angles of  $\beta = 0$  and  $180$  deg.

Figure 12 shows a plot of measured dominant wavelength vs relative surface shear stress magnitude. For  $\beta = 0$  deg, measured color change was seen to scale linearly with increasing  $\tau/\tau_r$  over the entire regime tested. At shear magnitudes beyond  $\tau/\tau_r = 8$ , only small additional decreases in  $\lambda_D$  were measured, i.e., this particular liquid crystal material experiences its full-spectrum, color-play response (orange to blue) in the shear range  $1 \leq \tau/\tau_r \leq 8$ . In marked contrast, the  $\beta = 180$  deg data set shows no color-play response over the same  $\tau/\tau_r$  range. However, note that although shear vectors with components directed toward the observer always appear as rusty red or brown, independent of surface shear stress magnitude, this characteristic of liquid crystal coatings renders them most valuable for dynamic visualization of regions of reverse flow.<sup>16</sup>

### Vector Measurement Methodology

The shear vector measurement methodology was derived directly from the results of Figs. 11 and 12. The four steps required to measure both the orientation  $\phi_r$  and the absolute magnitude  $\tau$  of an arbitrary surface shear stress vector beneath a three-dimensional flowfield are outlined next. To extend this method from a point-measurement technique to a full-surface (full-image) measurement technique, the fiber optic probe and spectrophotometer must be replaced by a three-chip, cosite sampled, red-green-blue (RGB) color video camera linked to a full-image frame grabber and a supporting computer. The correspondence between surface-point locations and image-pixel locations would have to be established for all  $\alpha_C$ ,  $\phi_C$  view-angle combinations used to record data. Calibration and data acquisition would then be accomplished in exactly the same manner as used in the point-measurement experiments.

### Step 1: Calibration

Successful utilization of the liquid crystal coating technique requires the user to select a mixture that has physical and optical properties consistent with the absolute shear levels to be encountered in the experiment. Viscosity of the mixture is the primary variable to consider. A mixture with an unacceptably low viscosity would tend to flow over/off the test surface under the applied shear, degrading the coating color-play response as well as causing flow-intrusive buildup, or "ridges," to form. Special surface treatments to counter this problem have been proposed.<sup>18</sup> A mixture with an unacceptably high viscosity would not exhibit a full-spectrum color-play response under the maximum applied shear, degrading the sensitivity of the measurement technique.

Once a coating of the proper viscosity has been applied to the surface (assumed planar at this point in the discussion), it is then illuminated with white light from the normal direction, and the maximum shear level of the experiment is applied.

The camera is positioned at a nominal above-plane view angle  $\alpha_C \sim 30$  deg, facing downstream relative to the nominal freestream velocity vector. The camera is then rotated about the test surface in circumferential-view angle  $\phi_C$ , holding  $\alpha_C$  constant, until the maximum color-change signal at the "calibration point" is recorded. This  $\phi$  orientation defines the calibration vector orientation  $\phi_C = \phi_r$ , i.e.,  $\beta = 0$  deg. At this orientation, the above-plane view angle  $\alpha_C$  should be adjusted (optimized) to maximize the color-change signal for the liquid crystal mixture in use and the shear magnitudes imposed on it. A single calibration curve of color (RGB signals converted to  $\lambda_D$  or hue) vs absolute shear stress magnitude, equivalent to the  $\beta = 0$ -deg curve of Fig. 12, must then be obtained; conventional point-measurement techniques<sup>1-3</sup> can be utilized for this purpose. It should be noted that for nonplanar test surfaces, a family of such color vs shear magnitude calibration curves would have to be generated to parametrically cover those effective, above-tangent-plane view angles encountered in the experiment. Sensitivity to off-normal illumination must also be quantified. Research in this area remains to be done.

Most importantly, the test methodology outlined herein does not require calibration curves at any  $\beta$  orientation other than the observer/vector aligned position at  $\beta = 0$  deg; it only requires the knowledge that the minimum dominant wavelength for any given shear stress magnitude occurs when the shear vector is aligned with, and directed away from, the observer. In other words, the set of curves represented by Fig. 11 is not required to apply the present measurement technique.

### Step 2: Data Acquisition

For  $\alpha_C$  maintained at the calibration setting, three or more full-surface images must be acquired at known  $\phi_C$  angles along a circumferential arc encompassing all possible vector directions to be encountered in the three-dimensional, steady-state flow under investigation. The three RGB voltages for every pixel in each image must be converted to a color value consistent with the calibration of step 1. It should be noted that extension of this method to unsteady flows would require that three or more fixed/synchronized cameras be positioned at circumferential-view angles encompassing the vector directions to be measured. Simultaneous full-field images would then provide freeze-frame records of the color-play response from each of these preset view angles. The color-play time responses of liquid crystal coatings subjected to shear stress vectors that vary with time in both magnitude and direction remain to be quantified.

### Step 3: Determination of Vector Directions

For each physical point on the surface, a curve fit of color vs circumferential-view angle  $\phi$  must be calculated using the data set acquired in step 2; functions that are symmetric about the "minimum-color" value are required, e.g., Gaussian or parabolic. Figure 13 provides examples of this procedure. The curve fit is then used to calculate the minimum-color value and the  $\phi$  angle at which it occurs, thereby defining the vector orientation  $\phi_r$ .

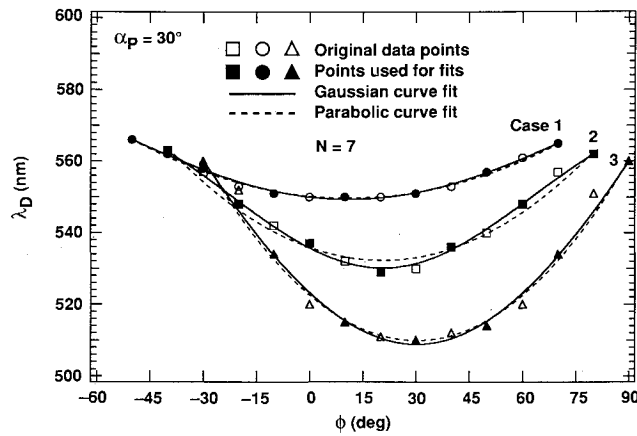


Fig. 13 Seven-point curve fits of dominant wavelength vs circumferential-view angle for test case vectors.

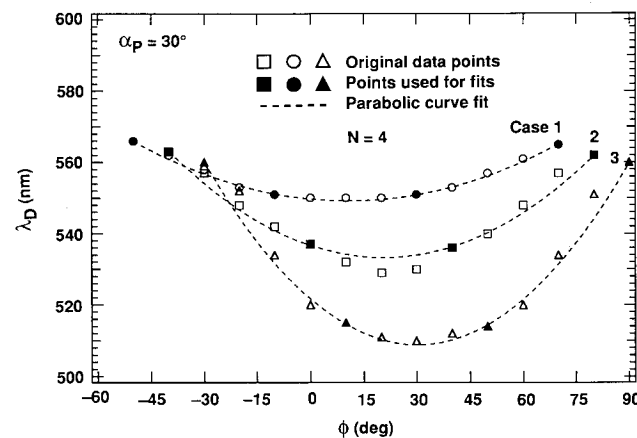


Fig. 14 Four-point curve fits of dominant wavelength versus circumferential-view angle for test case vectors.

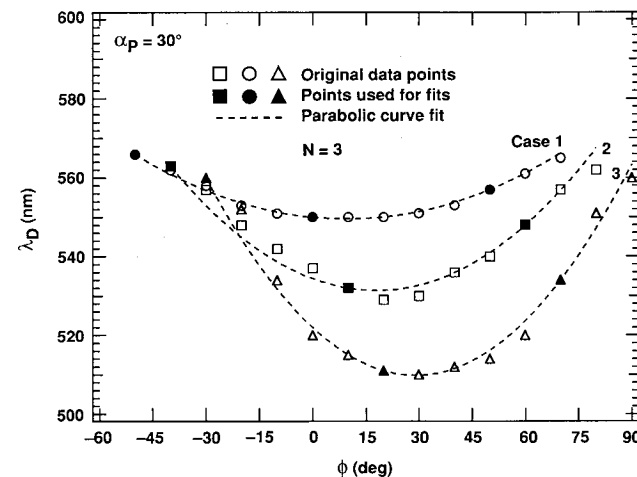


Fig. 15 Three-point curve fits of dominant wavelength vs circumferential-view angle for test case vectors.

#### Step 4: Determination of Vector Magnitudes

For each physical point on the surface, the curve-fit defined value of color at the vector orientation determined in step 3 is then input to the color vs shear magnitude calibration curve of step 1 to define the vector magnitude  $\tau$ .

#### Test-Case Vectors

Three separate experiments were conducted using the apparatus of Fig. 3 to illustrate the resolution achievable with this new tech-

Table 1 Test case vectors

Case	1	2	3
$\phi_r$ , deg	10	20	30
$\tau/\tau_r$	2.70	5.20	7.46

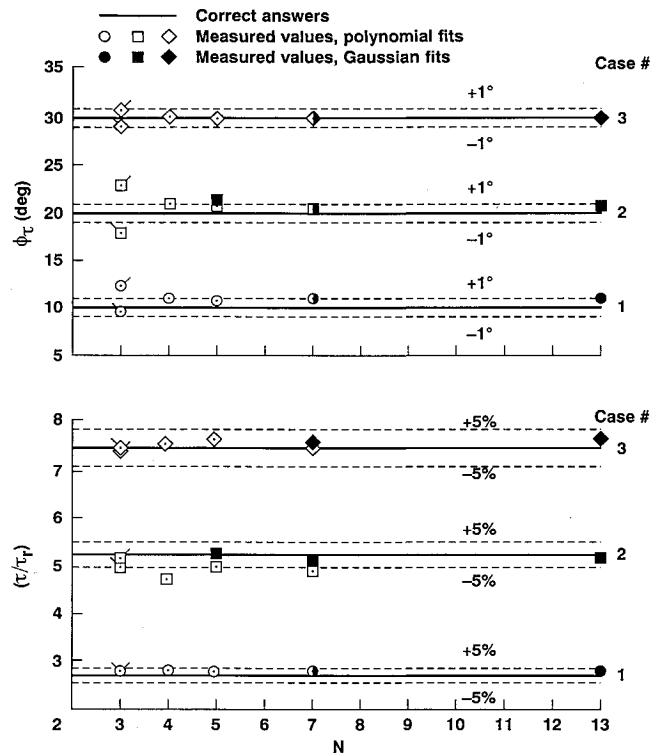


Fig. 16 Surface shear stress vector orientations and relative magnitudes vs number of data points used in curve fits; test case measured values in comparison to correct answers.

nique. In each experiment, 13 measurements were taken of  $\lambda_D$ , one every 10 deg in  $\phi$ , along an arc encompassing the known vector direction. The complete data sets for each test-case vector are shown in Figs. 13–15. Table 1 lists set values for the vector orientations; relative shear magnitudes were determined, in each case, from the measured  $\lambda_D$  value at  $\phi_P = \phi_r$  and the  $\beta = 0$ -deg calibration curve of Fig. 12.

A sensitivity study was then undertaken to define uncertainties in measured  $\phi_r$  and  $\tau/\tau_r$  values as a function of the number of data points used in the curve-fitting procedure and the equation applied. The influences of data scatter in the primary measurements of  $\lambda_D$  and  $\phi_P$  are also implicitly included in this resolution-determination task. In Fig. 13, 7 of the 13 available data points, including the “correct-answer” data points, were used; both second-order polynomial and Gaussian equations were applied. In Fig. 14, only four of the available data points were used in the polynomial fits for each case, and none of these was closer than 20 deg to the true minimum of its particular data set. In the limit, only three data points were used to define the second-order polynomial fits (see Fig. 15). Here, the middle data point of each set of three was purposely chosen to be 10 deg to the left of the true minimum. This three-point curve-fitting procedure was repeated using a middle data point 10 deg to the right of the true minimum in each case. These  $N = 3$  results are differentiated by the left and right flagged data symbols in Fig. 16.

Figure 16 summarizes the results of the sensitivity study. Use of  $N \geq 5$  and Gaussian curve fits yielded measured vector orientations within  $\pm 1$  deg of the correct answers and measured vector magnitudes within  $\pm 5\%$  of the correct answers in all cases. Use of  $N \leq 7$  and second-order polynomial curve fits yielded measured vector

orientations that were within  $\pm 1$  deg of the correct answers for 12 out of 15 attempts; worst-case discrepancies were 2–3 deg for  $N = 3$ , case 2. Corresponding measurements of vector magnitudes were within  $\pm 5\%$  of the correct answers in 12 out of 15 attempts; worst-case discrepancies were 9–10% for  $N = 4$ , case 2.

### Summary

1) Color video images of liquid crystal coatings subjected to surface shear stress vectors of known direction showed that, under normal white-light illumination and oblique observation, any point exposed to a shear vector with a component directed away from the observer exhibited a color-play response. This color-play response was characterized by a shift from the no-shear orange color toward the blue end of the visible spectrum, with the extent of the color change being a function of shear magnitude. Conversely, any point exposed to a shear vector with a component directed toward the observer exhibited a noncolor-play response, always characterized by a rusty red or brown color, independent of shear magnitude. These combined color-play characteristics of liquid crystal coatings render them most valuable for visualization of dynamic flow reversals or flow divergences.

2) Liquid crystal coating color-play responses to changes in relative surface shear stress magnitude and to changes in relative in-plane view angle between the vector and observer were quantified using a fiber optic probe and spectrophotometer. Measurements of spectral scattering intensity were taken at a point on the centerline of a turbulent wall jet flow. For a given shear stress magnitude, the minimum dominant wavelength or maximum color change was always measured when the shear vector was aligned with, and directed away from, the probe line of sight. Changes in relative in-plane view angle to either side of this vector/observer aligned position resulted in symmetric Gaussian increases in measured dominant wavelength. For this vector/observer aligned orientation, color change was found to scale linearly with increasing shear stress magnitude over an eight-fold range.

Based on these observations and spectral data, a surface shear stress vector measurement methodology was devised. For a fixed above-plane view angle, color measurements taken along several different in-plane lines of sight could be curve fit against in-plane view angle and used to define the maximum color-change orientation, i.e., the vector direction; the extent of the color change occurring at the vector orientation could then be used to define the vector magnitude. Based on initial tests, the measurement resolution of this technique was found to be  $\pm 1$  deg for vector orientation and  $\pm 5\%$  for vector magnitude. An approach to extend the present methodology to full-surface applications has been proposed.

### Acknowledgments

The efforts of the following individuals are gratefully acknowledged: NASA Ames Graduate Student Researchers Dino Farina of Stanford University and Tim Haynes of Arizona State University for their assistance in data acquisition and reduction; Christine Gong of Sterling Software Company and Jay Scheibe of Pulsar Video for their assistance in video frame grabbing and video editing.

### References

- <sup>1</sup>Hanratty, T. J., and Campbell, J. A., "Measurement of Wall Shear Stress," *Fluid Mechanics Measurements*, Hemisphere, Washington, DC, 1983, pp. 559–615.
- <sup>2</sup>Haritonidis, J. H., "The Measurement of Wall Shear Stress," *Advances in Fluid Mechanic Measurements*, Springer-Verlag, New York, 1989, pp. 229–261.
- <sup>3</sup>Diller, T. E., and Telionis, D. P., "Time-Resolved Heat Transfer and Skin Friction Measurements in Unsteady Flow," *Advances in Fluid Mechanic Measurements*, Springer-Verlag, New York, 1989, pp. 323–355.
- <sup>4</sup>Ferguson, J. L., "Liquid Crystals," *Scientific American*, Vol. 211, Aug. 1964, pp. 76–85.
- <sup>5</sup>Klein, E. J., "Liquid Crystals in Aerodynamic Testing," *Astronautics and Aeronautics*, Vol. 6, July 1968, pp. 70–73.
- <sup>6</sup>Reda, D. C., "Observations of Dynamic Stall Phenomena Using Liquid Crystal Coatings," *AIAA Journal*, Vol. 29, No. 2, 1991, pp. 308–310.
- <sup>7</sup>Hall, R. M., Obara, C. J., Carraway, D. L., Johnson, C. B., Wright, E. J., Covell, P. F., and Azzazy, M., "Comparisons of Boundary-Layer Transition Measurement Techniques at Supersonic Mach Numbers," *AIAA Journal*, Vol. 29, No. 6, 1991, pp. 865–871.
- <sup>8</sup>Reda, D. C., and Aeschliman, D. P., "Liquid Crystal Coatings for Surface Shear-Stress Visualization in Hypersonic Flows," *Journal of Spacecraft and Rockets*, Vol. 29, No. 2, 1992, pp. 155–158.
- <sup>9</sup>Holmes, B. J., Gall, P. D., Croom, C. C., Manuel, G. S., and Kelliher, W. C., "A New Method for Laminar Boundary Layer Transition Visualization in Flight: Color Changes in Liquid Crystal Coatings," NASA TM-87666, Jan. 1986.
- <sup>10</sup>Klein, E. J., and Margozi, A. P., "Exploratory Investigation on the Measurement of Skin Friction by Means of Liquid Crystals," NASA TM-X-1774, May 1969.
- <sup>11</sup>Gaudet, L., and Gell, T. G., "Use of Liquid Crystals for Qualitative and Quantitative 2-D Studies of Transition and Skin Friction," Royal Aerospace Establishment, TM AERO-2159, London, June 1989.
- <sup>12</sup>Bonnett, P., Jones, T. V., and McDonnell, D. G., "Shear-Stress Measurement in Aerodynamic Testing Using Cholesteric Liquid Crystals," *Liquid Crystals*, Vol. 6, No. 3, 1989, pp. 271–280.
- <sup>13</sup>Toy, N., Savory, E., and Paskin, S., "The Development of a System for Real-Time, Full-Field Surface Shear Stress Measurements Using Liquid Crystals," *Proceedings of the 12th Symposium on Turbulence*, University of Missouri—Rolla, Rolla, MO, 1990, pp. B15-1–B15-8.
- <sup>14</sup>Parmar, D. S., "A Novel Technique for Response Function Determination of Shear Sensitive Cholesteric Liquid Crystals for Boundary Layer Investigations," *Review of Scientific Instruments*, Vol. 62, No. 6, 1991, pp. 1596–1608.
- <sup>15</sup>Toy, N., Savory, E., and Disimile, P. J., "Determination of Surface Temperature and Surface Shear Stress Using Liquid Crystals," *Proceedings, Forum on Turbulent Flows*, ASME/JSME Joint Fluids Engineering Conf. (Portland, OR), American Society of Mechanical Engineers, New York, 1991, pp. 39–44.
- <sup>16</sup>Reda, D. C., Muratore, J. J., Jr., and Heineck, J. T., "Time and Flow-Direction Responses of Shear-Stress-Sensitive Liquid Crystal Coatings," *AIAA Journal*, Vol. 32, No. 4, 1994, pp. 693–700.
- <sup>17</sup>Padmanabham, G., and Lakshmana Gowda, B. H., "Mean and Turbulence Characteristics of a Class of Three-Dimensional Wall Jets—Part 1: Mean Flow Characteristics," *Journal of Fluids Engineering*, Vol. 113, Dec. 1991, pp. 620–628.
- <sup>18</sup>Parmar, D. S., Singh, J. J., and Eftekhari, A., "A Shear Sensitive Monomer-Polymer Liquid Crystal System for Wind Tunnel Applications," *Review of Scientific Instruments*, Vol. 63, No. 1, 1992, pp. 225–229.
- <sup>19</sup>Wyszecki, G., "Colorimetry," *Handbook of Optics*, McGraw-Hill, New York, 1978, Sec. 9, pp. 9-1–9-40.
- <sup>20</sup>Kasagi, N., Moffat, R. J., and Hirata, M., "Liquid Crystals," *Handbook of Flow Visualization*, Hemisphere, New York, 1989, Chap. 8, pp. 105–124.
- <sup>21</sup>Camci, C., Kim, K., and Hippensteel, S. A., "A New Hue Capturing Technique for the Quantitative Interpretation of Liquid Crystal Images Used in Convective Heat Transfer Studies," *Journal of Turbomachinery*, Vol. 114, No. 10, 1992, pp. 765–775.